Publishing House
AKAPIT

COMPUTER METHODS IN MATERIALS SCIENCE

Informatyka w Technologii Materiałów

Vol. 15, 2015, No. 1

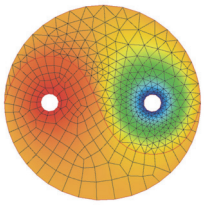

CRACK ANALYSES IN CONDUCTING AND NON-CONDUCTING PIEZOELECTRIC SOLIDS

JAN SLADEK[1]*, VLADIMIR SLADEK[1], MILAN ZMINDAK[2], SLAVOMIR HRCEK[2]

[1] Institute of Construction and Architecture, Slovak Academy of Sciences, 84503 Bratislava, Slovakia
[2] Faculty of Mechanical Engineering, University of Zilina, 01026 Zilina, Slovakia
**Corresponding author: sladek@savba.sk*

Abstract

The stress intensity factor and electric displacement intensity factor for cracks in conducting and non-conducting piezoelectric materials is investigated. Transient dynamic crack problems are analyzed. The coupled governing partial differential equations (PDE) for stresses, electric displacement field and electric current are satisfied in a local weak-form on small fictitious subdomains. Local integral equations are derived for a unit function as the test function on circular subdomains. All field quantities are approximated by the moving least-squares (MLS) scheme. The influence of the electric conductivity on the stress intensity and electric intensity factors is shown in numerical examples for an edge crack in a finite strip under a pure mechanical impact load with Heaviside time variation.

Key words: meshless approximation, local integral equations, intensity factors, impermeable boundary conditions

1. INTRODUCTION

Piezoelectric materials (PE) can be either dielectrics or semiconductors. Up to date dielectric materials are more intensively investigated than semiconductors since dielectric materials are described by simpler governing equations. The solution of the boundary value problems for coupled electro-mechanical problems requires advanced numerical methods due to the high mathematical complexity. Piezoelectric materials are brittle and they have a tendency to develop cracks even in manufacture process. Therefore, it is important to understand fracture of piezoelectric ceramics. Pak (1990) obtained the closed-form solutions for an infinite PE medium under an anti-plane loading by using a complex variable method. Later, Park and Sun (1995) obtained closed-form solutions for all the three fracture modes associated with a crack in an infinite PE medium. They investigated the effects of the electric field on the fracture of PE ceramics. General computational methods like the finite element method (FEM) (Gruebner et al., 2003; Govorukha & Kamlah, 2004; Enderlein et al., 2005; Kuna, 2006) and the boundary element method (BEM) (Pan, 1999; Davi & Milazzo, 2001; Gross et al., 2005; Garcia-Sanchez et al., 2005, 2007) need to be applied for general crack analyses in PE solids. In recent years, meshless formulations are becoming popular due to their high adaptability and low costs in preparation of input and output data for numerical analyses. Even continuously varying PE material properties are considered in some numerical analyses for non-conducting dielectric PE (Sladek et al., 2007).

In piezoelectric semiconductors (conducting PE) the induced electric field produces also the electric current. The interaction between mechanical fields and mobile charges in piezoelectric semiconductors is called the acoustoelectric effect (Hutson & White, 1962; White, 1962). An acoustic wave traveling in a PE semiconductor can be amplified by application

ISSN 1641-8581

of an initial or biasing dc electric field (Yang & Zhou, 2005). There are only few papers devoted to crack problems in piezoelectric semiconductor materials. These papers concerned only the anti-plane crack problem in unbounded domain with a semi-infinite crack (Yang, 2005) or a finite crack (Hu et al., 2007) under stationary conditions. The Fourier transform technique was applied to reduce the problem to a pair of dual integral equations.

In the present paper, we aim at analyzing the in-plane crack problem in bounded domains under a mechanical and electric load. Static and transient boundary conditions are considered here. The meshless Petrov-Galerkin (MLPG) method (Sladek et al., 2013) is developed for the solution of the initial-boundary value problems in conducting piezoelectric solids. Nodal points are introduced and spread on the analyzed domain and each node is surrounded by a small circle for simplicity, but without loss of generality. The spatial variations of the displacement, electric potential and electron density are approximated by the moving least-squares (MLS) scheme. After performing the spatial integrations, a system of ordinary differential equations for unknown nodal values is obtained. The essential boundary conditions on the global boundary are satisfied by the collocation.

2. LOCAL INTEGRAL EQUATIONS AND NUMERICAL SOLUTION

Consider a homogeneous piezoelectric semiconductor with electron density M_0 in the unloaded state and vanishing initial electric field E_0. The quasi-static approximation can be supposed for electromagnetic fields, since the frequency of external loadings is assumed to be significantly lower than the characteristic frequency of the electromagnetic fields. Then, the governing equations within the linear theory are given by the balance of momentum, Gauss's law and conservation of the electric charge (Hutson & White, 1962)

$$\sigma_{ij,j}(\mathbf{x},\tau)=\rho\ddot{u}_i(\mathbf{x},\tau), \qquad D_{i,i}(\mathbf{x},\tau)=qM(\mathbf{x},\tau), \qquad q\dot{M}(\mathbf{x},\tau)+J_{i,i}=0\ , \tag{1}$$

where $\ddot{u}_i$, σ_{ij} , D_i, and q are the acceleration of elastic displacements, stress tensor, electric displacement field, and electric charge of electron, respectively. The electron density and electric current are denoted by M and J_i, respectively. Symbol ρ is used for the mass density.

The constitutive equations are given as (Hutson & White, 1962; White, 1962)

$$\sigma_{ij}(\mathbf{x},\tau)=c_{ijkl}\varepsilon_{kl}(\mathbf{x},\tau)-e_{kij}E_k(\mathbf{x},\tau),$$
$$D_j(\mathbf{x},\tau)=e_{jkl}\varepsilon_{kl}(\mathbf{x},\tau)+h_{jk}E_k(\mathbf{x},\tau),$$
$$J_i(\mathbf{x},\tau)=qM_0\mu_{ij}(\mathbf{x})E_j(\mathbf{x},\tau)-qd_{ij}M_{,j}(\mathbf{x},\tau), \tag{2}$$

where c_{ijkl}, e_{ijk}, h_{ij}, μ_{ij} and d_{ij} are the elastic, piezoelectric, dielectric, electron mobility and carrier diffusion material coefficients, respectively.

The strain tensor ε_{ij} and the electric field vector E_j are related to the displacements u_i and the electric potential ϕ by

$$\varepsilon_{ij}=\frac{1}{2}\left(u_{i,j}+u_{j,i}\right), \quad E_j=-\phi_{,j}\ . \tag{3}$$

According to the meshless local Petrov-Galerkin (MLPG) method, we construct a weak-form of (1) over the local subdomains Ω_s around each node $\mathbf{x}^i$ inside the global domain Ω (Sladek et al., 2013). The subdomains are distributed in the analyzed domain. The local subdomains could be of any geometrical shape and size. For the sake of simplicity, the local subdomains are taken here to be of a circular shape. For this case, the evaluation of domain-integrals is quite easy. The local weak form of the governing equations (1) can be written as

$$\int_{\Omega_s}\left[\sigma_{ij,j}(\mathbf{x},\tau)-\rho\ddot{u}_i(\mathbf{x},\tau)\right]u^*_{ik}(\mathbf{x})\,d\Omega\ =0\,, \tag{4}$$

where $u^*_{ik}(\mathbf{x})$ is a test function and $\Omega_s\subset\Omega$.

Applying the Gauss divergence theorem to the first integral and choosing the Heaviside step function as the test function $u^*_{ik}(\mathbf{x})$ in each subdomain

$$u^*_{ik}(\mathbf{x})=\begin{cases}\delta_{ik} & \text{at}\quad \mathbf{x}\in\Omega_s\\ 0 & \text{at}\quad \mathbf{x}\notin\Omega_s\end{cases}$$

the local weak-form (4) is converted into the following local boundary-domain integral equations

$$\int_{L_s+\Gamma_{su}}t_i(\mathbf{x},\tau)d\Gamma-\int_{\Omega_s}\rho\ddot{u}_i(\mathbf{x},\tau)d\Omega=-\int_{\Gamma_{st}}\tilde{t}_i(\mathbf{x},\tau)d\Gamma\ , \tag{5}$$

where the boundary of the local subdomain $\partial\Omega_s$ consists of three parts $\partial\Omega_s=L_s\cup\Gamma_{st}\cup\Gamma_{su}$ (Sladek et al., 2013). Here, L_s is the local boundary that is totally inside the global domain, Γ_{st} is the part of the local boundary which coincides with the global trac-

tion boundary, i.e., $\Gamma_{st} = \partial\Omega_s \cap \Gamma_t$, and Γ_{su} is the part of the local boundary that coincides with the global displacement boundary, i.e., $\Gamma_{su} = \partial\Omega_s \cap \Gamma_u$. Similar definitions are valid also for other fields and related integration parts.

The local integral equation (5) is valid for both the homogeneous and nonhomogeneous solids. Nonhomogeneous material properties are included in equation (5) through the elastic and piezoelectric coefficients involved in the traction components

$$t_i(\mathbf{x},\tau) = \left[c_{ijkl} u_{k,l}(\mathbf{x},\tau) + e_{kij} \phi_{,k}(\mathbf{x},\tau) \right] n_j(\mathbf{x}) .$$

The local integral equation corresponding to the second governing equation in (1) has the following form

$$\int_{L_s+\Gamma_{sp}} Q(\mathbf{x},\tau) d\Gamma - \int_{\Omega_s} qM(\mathbf{x},\tau) d\Omega = -\int_{\Gamma_{sq}} \tilde{Q}(\mathbf{x},\tau) d\Gamma \tag{6}$$

where

$$Q(\mathbf{x},\tau) = D_j(\mathbf{x},\tau) n_j(\mathbf{x}) = \left[e_{jkl} u_{k,l}(\mathbf{x},\tau) - h_{jk} \phi_{,k}(\mathbf{x},\tau) \right] n_j .$$

Finally, the local integral equation corresponding to the last governing equation in (1) has the form

$$\int_{L_s+\Gamma_{sa}} S(\mathbf{x},\tau) d\Gamma + \int_{\Omega_s} q\dot{M}(\mathbf{x},\tau) d\Omega = -\int_{\Gamma_{sb}} \tilde{S}(\mathbf{x},\tau) d\Gamma \tag{7}$$

where the electric current flux is given by

$$S(\mathbf{x},\tau) = J_j(\mathbf{x},\tau) n_j(\mathbf{x}) =$$

$$\left[-qM_0 \mu_{kj} \phi_{,k}(\mathbf{x},\tau) - qd_{jk} M_{,k}(\mathbf{x},\tau) \right] n_j .$$

In the present paper the trial functions are approximated by the moving least squares (MLS) method on a number of nodes spread over the influence domain. According to the MLS (Sladek et al., 2013) method, the approximation of physical fields $\mathbf{f}(\mathbf{x},\tau)$ (mechanical displacements, the electric potential and electron density) over a number of randomly located nodes $\left\{ \mathbf{x}^a \right\}$, a = 1,2,…n, is given by

$$\mathbf{f}(\mathbf{x},\tau) = \boldsymbol{\pi}^T(\mathbf{x}) \mathbf{a}(\mathbf{x},\tau) , \tag{8}$$

where $\boldsymbol{\pi}^T(\mathbf{x}) = \left[\pi^1(\mathbf{x}), \pi^2(\mathbf{x}), ..., \pi^m(\mathbf{x}) \right]$ is a complete monomial basis of order m; and $\mathbf{a}(\mathbf{x},\tau)$ is a vector containing the coefficients $a^j(\mathbf{x},\tau)$, j = 1,2,…,m and $\mathbf{x} \equiv (x_1, x_3)$. The coefficient vector $\mathbf{a}(\mathbf{x},\tau)$ is determined by minimizing a weighted discrete L_2-norm defined as

$$J(\mathbf{x}) = \sum_{a=1}^{n} w^a(\mathbf{x}) \left[\boldsymbol{\pi}^T(\mathbf{x}^a) \mathbf{a}(\mathbf{x},\tau) - \hat{\mathbf{f}}^a(\tau) \right]^2 ,$$

where n is the number of nodes used for the approximation. It is determined by the weight function $w^a(\mathbf{x})$ associated with the node a. The stationarity of J with respect to $\mathbf{a}(\mathbf{x},\tau)$ leads to the following linear relation between $\mathbf{a}(\mathbf{x},\tau)$ and $\hat{\mathbf{f}}(\tau) = \left[\hat{\mathbf{f}}^1(\tau), ..., \hat{\mathbf{f}}^n(\tau) \right]^T$

$$\mathbf{A}(\mathbf{x}) \mathbf{a}(\mathbf{x},\tau) - \mathbf{B}(\mathbf{x}) \hat{\mathbf{f}}(\tau) = 0 , \tag{9}$$

where

$$\mathbf{A}(\mathbf{x}) = \sum_{a=1}^{n} w^a(\mathbf{x}) \boldsymbol{\pi}(\mathbf{x}^a) \boldsymbol{\pi}^T(\mathbf{x}^a) ,$$

$$\mathbf{B}(\mathbf{x}) = \left[w^1(\mathbf{x}) \boldsymbol{\pi}(\mathbf{x}^1), w^2(\mathbf{x}) \boldsymbol{\pi}(\mathbf{x}^2), ..., w^n(\mathbf{x}) \boldsymbol{\pi}(\mathbf{x}^n) \right].$$

The solution of equation (9) for $\tilde{\mathbf{a}}(\mathbf{x},s)$ and the subsequent substitution into equation (8) lead to the following expression

$$\mathbf{u}^h(\mathbf{x},\tau) == \sum_{a=1}^{n} N^a(\mathbf{x}) \hat{\mathbf{u}}^a(\tau) ,$$

$$\phi^h(\mathbf{x},\tau) = \sum_{a=1}^{n} N^a(\mathbf{x}) \hat{\phi}^a(\tau) ,$$

$$M^h(\mathbf{x},\tau) = \sum_{a=1}^{n} N^a(\mathbf{x}) \hat{M}^a(\tau) , \tag{10}$$

where the nodal values, $\hat{\mathbf{u}}^a(\tau) = \left(\hat{u}_1^a(\tau), \hat{u}_3^a(\tau) \right)^T$, $\hat{\phi}^a(\tau)$, and $\hat{M}^a(\tau)$, are fictitious parameters for the displacements, electric potential and electron density, respectively, and

$$\mathbf{N}^T(\mathbf{x}) = \boldsymbol{\pi}^T(\mathbf{x}) \mathbf{A}^{-1}(\mathbf{x}) \mathbf{B}(\mathbf{x}) ,$$

$N^a(\mathbf{x})$ is the shape function associated with the node a. A 4th-order spline-type weight function is applied in the present work

$$w^a(\mathbf{x}) = \begin{cases} 1 - 6\left(\frac{d^a}{r^a}\right)^2 + 8\left(\frac{d^a}{r^a}\right)^3 - 3\left(\frac{d^a}{r^a}\right)^4, & 0 \le d^a \le r^a \\ 0, & d^a \ge r^a \end{cases} ,$$

where $d^a = \left\| \mathbf{x} - \mathbf{x}^a \right\|$ and r^a is the size of the support domain.

Then, the traction vector $t_i(\mathbf{x},\tau)$ at a boundary point $\mathbf{x} \in \partial\Omega_s$ is approximated in terms of the nodal displacements $\hat{\mathbf{u}}^a(\tau)$ and electric potentials $\hat{\phi}^a(\tau)$ as

$$\mathbf{t}^h(\mathbf{x},\tau) = \mathsf{N}(\mathbf{x})\mathbf{C}(\mathbf{x})\sum_{a=1}^{n}\mathbf{B}^a(\mathbf{x})\hat{\mathbf{u}}^a(\tau) + \mathsf{N}(\mathbf{x})\mathbf{L}(\mathbf{x})\sum_{a=1}^{n}\mathbf{P}^a(\mathbf{x})\hat{\phi}^a(\tau), \qquad (11)$$

where the matrices $\mathbf{C}(\mathbf{x})$, $\mathbf{L}(\mathbf{x})$ represent elastic constants and piezoelectric coefficients, respectively, the matrix $\mathsf{N}(\mathbf{x})$ is related to the normal vector $\mathbf{n}(\mathbf{x})$ on $\partial\Omega_s$ by

$$\mathsf{N}(\mathbf{x}) = \begin{bmatrix} n_1 & 0 & n_3 \\ 0 & n_3 & n_1 \end{bmatrix},$$

and finally, the matrices $\mathbf{B}^a$ and $\mathbf{P}^a$ represent the gradients of the shape functions as

$$\mathbf{B}^a(\mathbf{x}) = \begin{bmatrix} N^a_{,1} & 0 \\ 0 & N^a_{,3} \\ N^a_{,3} & N^a_{,1} \end{bmatrix}, \qquad \mathbf{P}^a(\mathbf{x}) = \begin{bmatrix} N^a_{,1} \\ N^a_{,3} \end{bmatrix}.$$

Symbols $n_1(\mathbf{x})$ and $n_3(\mathbf{x})$ are components of the normal vector $\mathbf{n}(\mathbf{x})$ to the boundary $\partial\Omega_s$ at the Gaussian point $\mathbf{x}$ in plane $x_1 - x_3$.

Similarly one can write

$$Q^h(\mathbf{x},\tau) = \mathbf{N}_1(\mathbf{x})\mathbf{G}(\mathbf{x})\sum_{a=1}^{n}\mathbf{B}^a(\mathbf{x})\hat{\mathbf{u}}^a(\tau) - \mathbf{N}_1(\mathbf{x})\mathbf{H}(\mathbf{x})\sum_{a=1}^{n}\mathbf{P}^a(\mathbf{x})\hat{\phi}^a(\tau), \qquad (12)$$

where the matrices $\mathbf{G}(\mathbf{x})$ and $\mathbf{H}(\mathbf{x})$ represent piezoelectric and dielectric coefficients and

$$\mathbf{N}_1(\mathbf{x}) = \begin{bmatrix} n_1 & n_3 \end{bmatrix}.$$

Finally, the electric current flux $\mathbf{S}(\mathbf{x},\tau)$ is approximated by

$$S^h(\mathbf{x},\tau) = -\mathbf{N}_1(\mathbf{x})qM_0\mathbf{A}(\mathbf{x})\sum_{a=1}^{n}\mathbf{P}^a(\mathbf{x})\hat{\phi}^a(\tau) - \mathbf{N}_1(\mathbf{x})q\mathbf{F}(\mathbf{x})\sum_{a=1}^{n}\mathbf{P}^a(\mathbf{x})\hat{M}^a(\tau), \qquad (13)$$

with the matrices $\mathbf{A}(\mathbf{x})$, $\mathbf{F}(\mathbf{x})$ denoting electron mobility and carrier diffusion parameters.

Substituting the traction approximation (11), electric charge (12) and electric current (13) into the local integral equations (5)-(7) one obtains a system of ordinary differential equations for nodal quantities

$$\sum_{a=1}^{n}\left[\left(\int_{L_s+\Gamma_{st}} \mathsf{N}(\mathbf{x})\mathbf{C}(\mathbf{x})\mathbf{B}^a(\mathbf{x})d\Gamma\right)\hat{\mathbf{u}}^a(\tau) - \left(\int_{\Omega_s}\rho(\mathbf{x})N^a d\Omega\right)\ddot{\hat{\mathbf{u}}}^a(\tau)\right] +$$

$$\sum_{a=1}^{n}\left[\left(\int_{L_s+\Gamma_{st}} \mathsf{N}(\mathbf{x})\mathbf{C}(\mathbf{x})\mathbf{B}^a(\mathbf{x})d\Gamma\right)\hat{\mathbf{u}}^a(\tau) - \left(\int_{\Omega_s}\rho(\mathbf{x})N^a d\Omega\right)\ddot{\hat{\mathbf{u}}}^a(\tau)\right] +$$

$$+\sum_{a=1}^{n}\left(\int_{L_s+\Gamma_{st}} \mathsf{N}(\mathbf{x})\mathbf{L}(\mathbf{x})\mathbf{P}^a(\mathbf{x})d\Gamma\right)\hat{\phi}^a(\tau) = -\int_{\Gamma_{st}}\tilde{\mathbf{t}}(\mathbf{x},\tau)d\Gamma \qquad (14)$$

$$\sum_{a=1}^{n}\left(\int_{L_s+\Gamma_{sq}} \mathbf{N}_1(\mathbf{x})\mathbf{G}(\mathbf{x})\mathbf{B}^a(\mathbf{x})d\Gamma\right)\hat{\mathbf{u}}^a(\tau) -$$

$$\sum_{a=1}^{n}\left(\int_{L_s+\Gamma_{sq}} \mathbf{N}_1(\mathbf{x})\mathbf{H}(\mathbf{x})\mathbf{P}^a(\mathbf{x})d\Gamma\right)\hat{\phi}^a(\tau) -$$

$$-\sum_{a=1}^{n}\left(\int_{\Omega_s} qN^a(\mathbf{x})d\Omega\right)\hat{M}^a(\tau) = -\int_{\Gamma_{sq}}\tilde{Q}(\mathbf{x},\tau)d\Gamma, \qquad (15)$$

$$-\sum_{a=1}^{n}\left(\int_{L_s+\Gamma_{sb}} \mathbf{N}_1(\mathbf{x})qM_0\mathbf{A}(\mathbf{x})\mathbf{P}^a(\mathbf{x})d\Gamma\right)\hat{\phi}^a(\tau) -$$

$$^a(\tau) - \sum_{a=1}^{n}\left(\int_{L_s+\Gamma_{sb}} \mathbf{N}_1(\mathbf{x})q\mathbf{F}(\mathbf{x})\mathbf{P}^a(\mathbf{x})d\Gamma\right)\hat{M}^a(\tau) +$$

$$+\sum_{a=1}^{n}\left(\int_{\Omega_s} qN^a(\mathbf{x})d\Omega\right)\dot{\hat{M}}^a(\tau) = -\int_{\Gamma_{sb}}\tilde{S}(\mathbf{x},\tau)d\Gamma. \qquad (16)$$

Above given system of ordinary differential equations is solved numerically by the Houbolt method.

The stress intensity factors (SIF) and electric displacement intensity factor (EDIF) K_N are computed numerically from the asymptotic expansion of displacements and electric potential at the crack tip vicinity

$$u_i(r,\theta) = \sqrt{\frac{2r}{\pi}} \sum_{N=1}^{4} K_N d_i^N(\theta) \quad ,$$

$$\phi(r,\theta) = \sqrt{\frac{2r}{\pi}} \sum_{N=1}^{4} K_N v^N(\theta) \quad , \qquad (17)$$

where $d_i^N(\theta)$ and $v^N(\theta)$ are dependent on material properties and they are given by Park and Sun (1995).

3. NUMERICAL EXAMPLES

An edge crack in a finite strip is analyzed in the first example. Due to the symmetry with respect to x_1 only a half of the specimen is modelled with the boundary conditions and discretization nodes being shown schematically in figure1. The geometry parameters are specified as: a = 0.5 m, a/w = 0.4 and h/w = 1.2. The material properties correspond to aluminum nitride (AlN) (Auld, 1973).

Electrically impermeable boundary conditions are assumed on crack faces. The strip is subjected to a pure mechanical load with Heaviside time variation and the intensity σ_0 = 1 Pa.

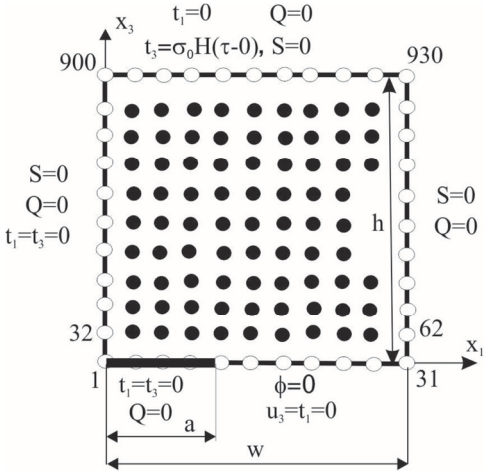

Fig. 1. *Edge crack in a finite homogeneous strip.*

We have used 930 nodes equidistantly distributed for the MLS approximation of physical fields. The static stress intensity factor for the considered load and geometry is equal to K_I^{stat} = 2.642 Pam$^{1/2}$. The time evolution of the normalized SIF for the cracked strip under an impact pure mechanical load is presented in figure 2 and the normalized electrical displacement factor $\Lambda K_D/K_I^{stat}$ in figure 3, where $\Lambda = e_{33}/h_{33}$. While the electrical displacement intensity factor for a pure static mechanical load is zero, the EDIF is not in the dynamic case with a finite velocity of elastic wave propagation for a pure mechanical load.

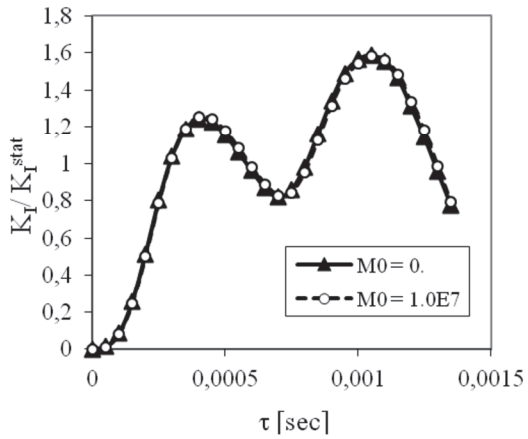

Fig. 2. *Normalized stress intensity factor for the edge crack in a strip under a pure mechanical load.*

One can observe that the initial electron density has a vanishing influence on the SIF. However, the EDIF is strongly dependent on the initial electron density. In the conducting PE the EDIF is enlarged with respect to that in non-conducting PE under a pure mechanical load. Accuracy of numerical results for non-conducting PE solids was tested in earlier published work (Sladek et al. 2007).

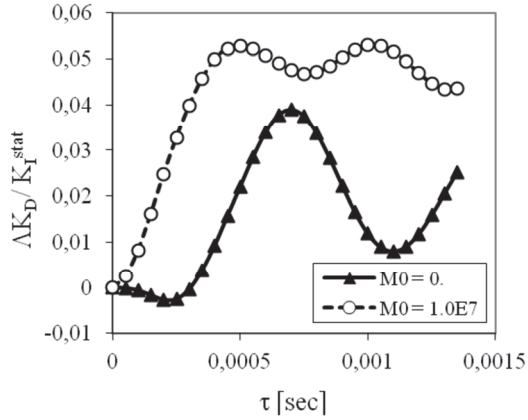

Fig. 3. *Normalized electrical displacement intensity factor for the edge crack in a strip under a pure mechanical load.*

ACKNOWLEDGEMENT

The authors gratefully acknowledge the supports by the Slovak Science and Technology Assistance Agency registered under number APVV-0014-10.

REFERENCES

Auld, B.A., 1973, *Acoustic Fields and Waves in Solids*, John Wiley and Sons, New York, 357-382.

Davi, G., Milazzo, A., 2001, Multidomain Boundary Integral Formulation for Piezoelectric Materials Fracture Mechanics, *Int J Solids Struct*, 38, 2557-2574.

Enderlein, M., Ricoeur, A., Kuna, M., 2005, Finite Element Techniques for Dynamic Crack Analysis in Piezoelectrics, *Int J Fracture*, 134, 191-208.

Garcia-Sanchez, F., Saez, A., Dominguez, J., 2005, Anisotropic and Piezoelectric Materials Fracture Analysis by BEM, *Comput Struct*, 83, 804-820.

Garcia-Sanchez, F., Zhang, Ch., Sladek, J., Sladek, V., 2007, 2-D Transient Dynamic Crack Analysis in Piezoelectric Solids by BEM, *Comp Mater Sci*, 39, 179-186.

Govorukha, V., Kamlah, M., 2004, Asymptotic Fields in the Finite Element Analysis of Electrically Permeable Interfacial Cracks in Piezoelectric Biomaterials, *Arch Appl Mech*, 74, 92-101.

Gross, D., Rangelov, T., Dineva, P., 2005, 2D Wave Scattering by a Crack in a Piezoelectric Plane Using Traction BIEM, *SID: Structural Integrity & Durability*, 1, 35-47.

Gruebner, O., Kamlah, M., Munz, D., 2003, Finite Element Analysis of Cracks in Piezoelectric Materials Taking into Account the Permittivity of the Crack Medium, *Eng Fract Mech*, 70, 1399-1413.

Hu, Y., Zeng, Y., Yang, J.S., 2007, A Mode III Crack in a Piezoelectric Semiconductor of Crystals with 6mm Symmetry, *Int J Solids Struct*, 44, 3928-3938.

Hutson, A.R., White, D.L., 1962, Elastic Wave Propagation in Piezoelectric Semiconductors, *J Appl Phys*, 33, 40-47.

Kuna, M. 2006, Finite Element Analyses of Cracks in Piezoelectric Structures – a Survey, *Arch Appl Mech*, 76, 725-745.

Pak, Y.E., 1990, Crack Extension Force in a Piezoelectric Material, *J Appl Mech*, 57, 647-653.

Pan, E., 1999, A BEM Analysis of Fracture Mechanics in 2D Anisotropic Piezoelectric Solids, *Eng Anal Bound Elem*, 23, 67-76.

Park, S.B., Sun, C.T., 1995, Effect of Electric Field on Fracture of Piezoelectric Ceramics, *Int J Fracture*, 70, 203-216.

Sladek, J., Stanak, P., Han, Z.D., Sladek, V., Atluri, S.N., 2013, Applications of the MLPG Method in Engineering & Sciences: A Review, *CMES-Comp Model Eng*, 92, 423-475.

Sladek, J., Sladek, V., Zhang, Ch., Solek, P., Pan, E., 2007, Evaluation of Fracture Parameters in Continuously Nonhomogeneous Piezoelectric Solids, *Int J Fracture*, 145, 313–326.

Yang, J.S., Zhou, H.G., 2005, Amplification of Acoustic Waves in Piezoelectric Semiconductor Plates, *Int J Solids Struct*, 42, 3171-3183.

Yang, J.S., 2005, An Anti-Plane Crack in a Piezoelectric Semiconductor, *Int J Fracture*, 136, 27-32.

White, D.L., 1962, Amplification of Ultrasonic Waves in Piezoelectric Semiconductors, *J Appl Phys*, 33, 2547-2554.

ANALIZA PROCESU PĘKANIA W PRZEWODZĄCYCH I NIEPRZEWODZĄCYCH MATERIAŁACH PIEZOELEKTRYCZNYCH

Streszczenie

W pracy badano współczynnik intensywności naprężeń i współczynnik intensywności przemieszczeń elektrycznych dla pękania w przewodzących i nieprzewodzących materiałach piezoelektrycznych. Analizowano problemy zmiennego, dynamicznego pękania. Sprzężone równania różniczkowe cząstkowe dla naprężeń, pola przemieszczeń elektrycznych i prądu elektrycznego zostały spełnione poprzez wprowadzenie słabej formy w małych, urojonych podobszarach. Lokalne równania całkowe zostały definiowane dla funkcji jednostkowej będącej funkcją testową w podobszarach. Wszystkie wielkości opisujące pole były aproksymowane z wykorzystaniem ruchomej metody najmniejszych kwadratów. Wpływ przewodności elektrycznej na intensywność naprężenia i współczynnik intensywności elektrycznej został pokazany w przykładach numerycznych pękania krawędzi w paśmie, które zostało poddane czystemu obciążeniu mechanicznemu będącemu funkcją czasu Heaviside'a.

Received: September 23, 2014
Received in a revised form: October 9, 2014
Accepted: December 17, 2014